Indian Journal of Chemistry
Vol. 57A, Aug-Sept 2018, pp. 1081-1090

Crystal engineering of molecular to nonmolecular metal malonates in presence of piperazine: Role of metal ions in tuning architectures

Kaustubh R Mote[†], Jency Thomas[‡,]* & Arunachalam Ramanan*

Department of Chemistry, Indian Institute of Technology Delhi, Hauz Khas, New Delhi 110 016, India

Email: aramanan@chemistry.iitd.ac.in (AR)/ jencythomas@stthomas.ac.in (JT)

Received 2 May 2018; revised and accepted 19 July 2018

Growth of transition metal malonate (mal) based solids from aqueous solution is investigated in the presence of piperazine (pip). Reaction under ambient conditions favored the growth of $[\{M(mal)_2(H_2O)_2\}\{H_2pip\}]$ (M: Ni, **1**; M: Co, **2**), $[\{Cu(mal)_2(H_2O)_2\}\{H_2pip\}].2H_2O$ (**3**), and, $[Zn(mal)(pip)(H_2O)]$ (**4**). While **1**-**3** are molecular solids, **4** is a 2-D coordination polymer. In the case of cobalt, higher acidic condition favored the formation of a molecular organic-inorganic salt, $[(H_2pip)\{CoCl_4\}]$ (**5**). The same reaction under a different crystallization condition, i.e., lesser polar solvent and slightly higher temperature (solvothermal) led to a 2-D coordination polymer $[\{Co(mal)(H_2O)(Hpip)\}]Cl$ (**6**). A retrosynthesis approach has been employed to interpret the crystallization reaction and compare the supramolecular reactivity of aggregating metal tectons in engineering the molecules to form either a molecular solid or coordination polymer.

Keywords: Crystallization, Transition metal ions, Malonate, Piperazine, Nickel, Cobalt, Copper, Zinc

Self-assembly of metal ions and organic ligands results in a variety of architectures ranging from discrete complexes to 3-D metal organic frameworks[1,2]. While the metal ion controls the directionality and coordination geometry, the ligand affects the flexibility and porosity in the solids[3]. A careful selection of the ligands and metal ion, as well as the reaction conditions (pH, solvent, temperature etc.) can lead to appropriately tuned architectures for possible applications in catalysis, conductivity, luminescence, magnetism and zeolitic behavior[4]. In this context, coordination polymers[5] are an important class of materials engineered by the metal coordination bonds by the appropriate choice of organic ligands.

Malonate (mal) is a versatile ligand capable of chelating a variety of metal ions; it can also function as bridging ligand between metal centers[6]. The stability of $\{M(mal)_2\}$ complex is mainly attributed to the formation of a stable six-membered ring and is found to be dependent on the metal ion. Among the divalent first-row transition metal ions, Cu(II) is known to form the strongest chelating complex with malonate. The strength of the bidentate chelating complexes of Co(II), Ni(II) and Zn(II) are of similar magnitude, but much smaller than that of Cu(II)[7]. The complexing ability of Cu(II) with malonate has been extensively studied in literature[8,9]. A majority of the known structures consist of a discrete anionic complex $\{Cu(mal)_2\}^{2-}$ that exhibits hydrogen bonding interactions with cationic species such as $\{M(H_2O)_6\}^{2+}$, M = Na(I), Zn(II), Cu(II), Ni(II), Co(II) and Mn(II)[10,11] or organic bases (as cations) such as aminopyridines, triethanolamine, monoethanolamine, diazacycloheptane[12,13]. Copper malonate also exists in several hydrated forms[14,15]. Relatively, a few structures are known with Co(II), Ni(II) and Zn(II)[16]. These consist of usually hydrogen bonded networks and 2-D networks stabilized by hydrogen bonding. On the other hand, diaza ligands can act as effective pillaring agents. Therefore, in this paper, we have examined the structural landscape of the metal malonates in the presence of piperazine (pip) which is a diaza ligand. Reaction under ambient condition favored the growth of $[\{M(mal)_2(H_2O)_2\}\{H_2pip\}]$ (M: Ni, **1**; M: Co, **2**), $[\{Cu(mal)_2(H_2O)_2\}\{H_2pip\}].2H_2O$ (**3**) and $[Zn(mal)(pip)(H_2O)]$ (**4**). While **1**-**3** are molecular solids, **4** is a 2-D coordination polymer. In the case of cobalt, more acidic condition favored the formation of a molecular organic/inorganic salt, $[(H_2pip)\{CoCl_4\}]$ (**5**). The same reaction under

[†]Present address: Tata Institute of Fundamental Research, Hyderabad, 500 107, India.

[‡]Present address: Research and PG Department of Chemistry, St. Thomas' College (Autonomous), Thrissur, Kerala 680 001, India.

solvothermal condition led to a 2-D coordination polymer [{Co(mal)(H_2O)(Hpip)}]Cl (**6**). We have employed a retrosynthesis approach to interpret the crystallization reaction and compare the supramolecular reactivity.

Materials and Methods

All reagents were of reagent grade and were used as received from commercial sources without further purification. Fourier transform infrared (FT-IR) spectra were recorded on KBr pellets using a Nicolet 5DX spectrophotometer. Thermogravimetric analysis (TGA) was done on Perkin-Elemer TGA7 from room temperature to 900 °C at a heating rate of 10 °C $min.^{-1}$ in nitrogen atmosphere to determine water and organic content as well as overall thermal stability of the product. Powder X-ray diffraction (PXRD) data was collected on a Bruker D8 Advance diffractometer using Ni-filtered Cu Kα radiation. Data was collected with a step size of 0.03° and count time of 2 s per step over the range $2° < 2\theta < 60°$.

Synthesis

To an aqueous solution of $MCl_2.xH_2O$ (4 mmol), malonic acid (8 mmol) was added with stirring. It resulted in a clear solution of pH ~1–2. An aqueous solution of piperazine (12 mmol) was further added. Upon mixing of the two solutions, the pH was found to be ~6–7. Subsequently, pH was adjusted by adding appropriate amount of 5 M HCl and the solution was left undisturbed until crystallization or precipitation was observed. Scheme 1 summarizes the synthetic protocol for the solids. Under highly acidic condition using cobalt chloride [{$CoCl_4$}{H_2pip}] (**5**) was obtained. Therefore the effect of solvent was further explored. Upon changing the solvent from water to methanol [{Co(mal)(H_2O)(Hpip)}Cl] (**6**) was isolated under hydrothermal condition. In a typical reaction, $CoCl_2.6H_2O$ (1.5 mmol), malonic acid (3 mmol) and piperazine (4.5 mmol) were taken in a bomb (10 mL capacity). 5.5 mL of methanol was added and the bomb was heated at 80 °C for three days. In all the cases, the yields were in the range of 70–80% based on the metal ion.

X-ray crystallography

X-ray diffraction studies of crystal mounted on a capillary, were carried out on a BRUKER AXS SMART-APEX diffractometer with a CCD area detector (Mo-Kα: 0.71073 Å, monochromator: graphite)[17]. Frames were collected at T = 298 K by ω, φ and 2θ rotation at 10 s per frame with SAINT[18]. The measured intensities were reduced to F2 and corrected for absorption with SADABS[18]. Structure solution, refinement, and data output were carried out with the SHELXTL program[19]. Non-hydrogen atoms were refined anisotropically. C-H hydrogen atoms were placed in geometrically calculated positions by using a riding model. O-H hydrogen atoms were localized by difference Fourier maps and refined in subsequent refinement cycles. Images were created with the DIAMOND program[20]. Hydrogen bonding interactions in the crystal lattice were calculated with SHELXTL and DIAMOND[19,20]. The crystal data and structure refinement of solids **1**–**6** are summarized in Table 1.

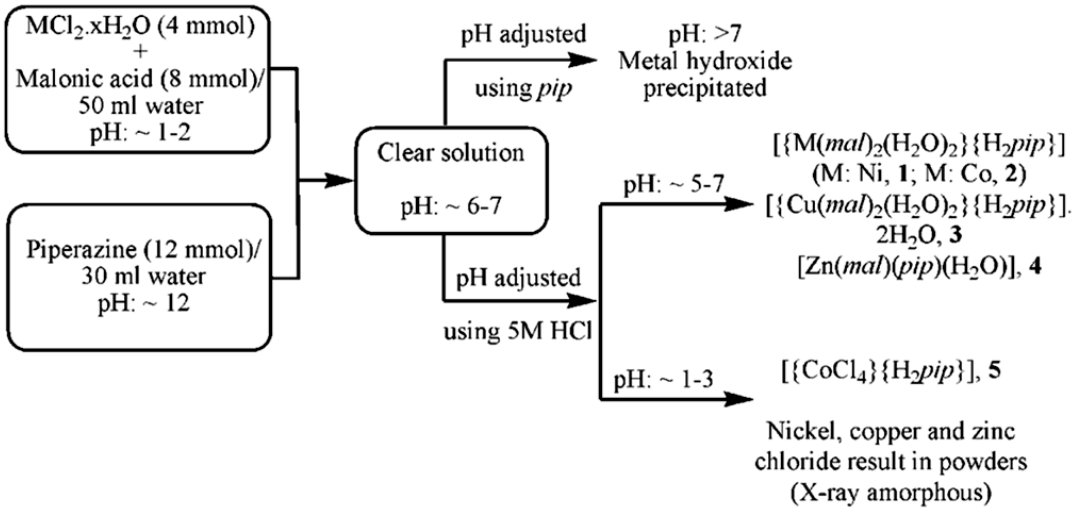

Experimental procedure to crystallize solids **1-5**

Scheme 1

Table 1 – Crystallographic details for solids **1-6**

	1	**2**	**3**	**4**	**5**	**6**
Formula	$C_{10}H_{20}N_2NiO_{10}$	$C_{10}H_{18}CoN_2O_{10}$	$C_{10}H_{16}CuN_2O_{12}$	$C_5H_9NO_5Zn$	$C_4H_{12}Cl_4CoN_2$	$C_7H_9ClCoN_3O_5$
Formula wt	386.97	385.19	419.80	228.52	288.89	309.55
T (K)	298(2)	298(2)	298(2)	298(2)	298(2)	298(2)
Space group	P-1	P-1	P-1	$P2_1/n$	$P2_12_12_1$	*Pnma*
a (Å)	7.0426(18)	7.0868(16)	6.219(2)	7.683(3)	8.2708(16)	22.634(11)
b (Å)	7.0545(18)	7.0916(16)	8.440(3)	6.545(2)	11.109(2)	7.454(4)
c (Å)	8.918(2)	8.896(2)	8.727(3)	14.293(5)	11.901(2)	6.985(4)
α (°)	108.151(4)	107.697(3)	80.522(5)	90	90	90
β (°)	101.396(3)	101.012(4)	70.990(4)	96.296(5)	90	90
γ (°)	108.609(4)	109.129(3)	82.199(5)	90	90	90
V (Å^3)	376.68(16)	380.85(15)	425.5(3)	714.4(4)	1093.5(3)	1178.4(11)
Z	2	2	2	4	4	4
d_{calc} (g cm^{-3})	1.706	1.679	1.638	2.125	1.755	1.745
$\mu_{Mo\ K\alpha}$ (cm^{-1})	1.344	1.182	1.348	3.418	2.493	1.696
λ (Å)	0.71073	0.71073	0.71073	0.71073	0.71073	0.71073
R_1(I>2σI), WR_2(all)	0.0277, 0.0718	0.0409, 0.1037	0.0365, 0.1073	0.0473, 0.0854	0.0655, 0.1305	0.0794, 0.1602
GOF	1.142	1.132	1.161	1.274	1.276	1.249
CCDC no.	717971	717972	717973	717974	857647	720736

Results and Discussion

Under highly acidic conditions (pH ~1–3) all reactions except for cobalt, resulted in amorphous powders; at pH ~5 and ~7, crystals were isolated in a week. PXRD pattern of the crystals confirmed that the same phase was obtained at pH ~5 and 7. At pH > 7, metal hydroxides precipitated in a week.

Crystal structure of $\{M(mal)_2(H_2O)_2\}(H_2pip)$ (M: Ni, 1; M: Co, 2)

$\{Ni(mal)_2(H_2O)_2\}(H_2pip)$, **1** and $\{Co(mal)_2(H_2O)_2\}\{H_2pip\}$, **2**, are isostructural molecular solids. Retrosynthesis of **1** or **2**, shows that the structure is built of the complex anion $\{M(mal)_2(H_2O)_2\}^{2-}$ and diprotonated cation, $\{H_2pip\}^{2+}$ interacting through noncovalent bonding (Fig. 1). Nickel or cobalt in the anionic complex occurs in a distorted octahedral coordination (Supplementary Data, Table S1). Hydrogen bonding between the aqua ligand and the uncoordinated oxygen atom of the carboxylate group leads to a 2-D lamellar structure in the *ab* plane. Strong N−H···O interactions mediated by $\{H_2pip\}^{2+}$ links the adjacent layers, such that C−H···O interactions between the carbon atoms on $\{H_2pip\}^{2+}$ and the carboxylate oxygen atoms provide further stability to this structure (Fig. 1 and Supplementary Data, Table S2). Thus, $\{H_2pip\}^{2+}$ units act as pillars between the H-bonded metal carboxylate sheets.

Crystal structure of $[\{Cu(mal)_2(H_2O)_2\}\{H_2pip\}].2H_2O$, 3

Like **1** and **2**, **3** is also a molecular solid but it occurs in the hydrated form. Retrosynthesis of **3** shows the occurrence of mediating water molecules (lattice water) apart from the anionic complex, $\{Cu(mal)_2(H_2O)_2\}^{2-}$ and the diprotonated cation (Fig. 2). As expected, the copper shows Jahn-Teller distortion with the apical Cu–O(W) bond length much longer (2.466(5) Å) than the equatorial plane (~1.95 Å). The average M–O bond length for the chelating malonate species follows the order: Cu–O < Ni–O < Co–O, which is consistent with the general coordination rules. In **3** also, the anions are arranged on a plane; however effective packing requires the mediation of water molecules. The interaction between a pair of adjacent complex anions, i.e., the aqua ligand, O1W of the first complex and the uncoordinated carboxylate oxygen, O2 of a second complex occurs via the lattice water, O2W. The overall arrangement leads to a 2-D lamellar structure (Fig. 2). In another direction (along *a*–axis), the structure can also be visualized as a chain of alternating $\{Cu(mal)_2(H_2O)_2\}$ and $\{H_2pip\}$ units interacting through a pair of N–H···O. Adjacent chains are linked through mediating water molecules (Fig. 3).

Crystal structure of $[Zn(mal)(pip)(H_2O)]$, 4

Unlike **1**–**3**, the nonmolecular solid **4** is an example of a 2-D coordination polymer (CP). Retrosynthesis of **4** suggests that this solid results from the supramolecular interaction of the two tectons[21], i.e., complex anion and unprotonated organic base. Unlike in solids **1-3**, the tecton is a 1:1 complex and hence a

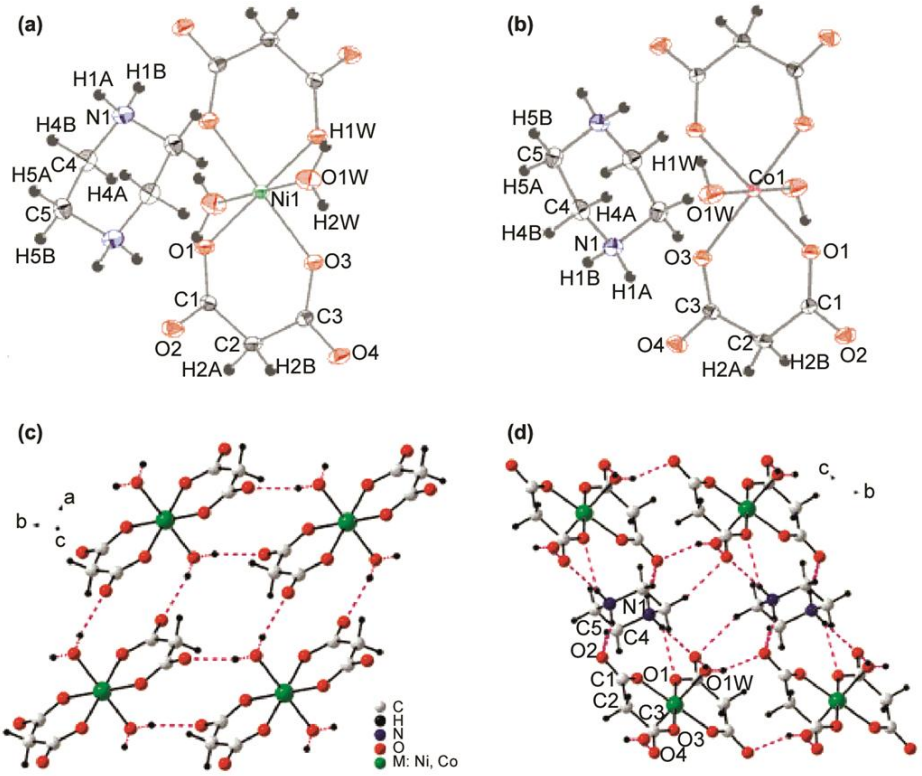

Fig. 1 – (a) ORTEP view of **1**, (b) ORTEP view of **2**, (c) H–bonding interaction (dashed purple lines) between $\{M(mal)_2(H_2O)_2\}^{2-}$ units between uncoordinated oxygen of carboxylate group and water molecule on metal center results in 2-D lamellar sheet, and, (d) the $\{H_2pip\}^{2+}$ units link the adjacent layers through N–H···O as well as C–H···O interactions.

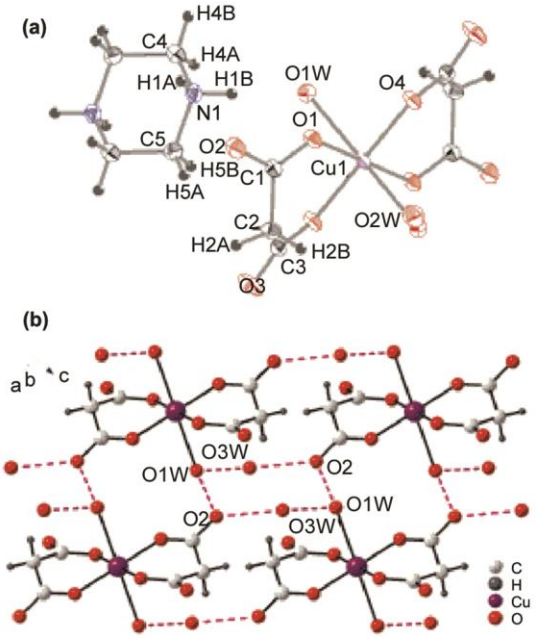

Fig. 2 – (a) ORTEP view of **3**, and, (b) view showing 2-D H-bonded sheet. [H-bonding interaction between $\{Cu(mal)_2(H_2O)_2\}^{2-}$ units between uncoordinated oxygen of carboxylate group and water molecule on metal center along with lattice water, O2W results in 2-D lamellar sheet (O1W…O2: 2.745(8); O2…O2W: 2.774(10); O3W…O1W: 2.743(10) Å)].

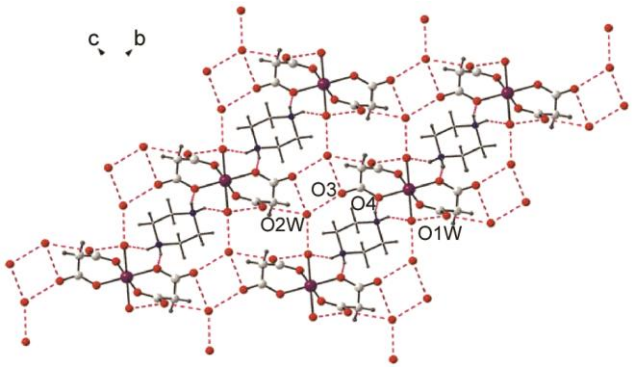

Fig. 3 – Along *a*-axis, alternating $\{Cu(mal)_2(H_2O)_2\}$ and $\{H_2pip\}$units interact through two pairs of N-H···O interactions forming chains. [Adjacent chains are linked through mediating water molecules O2W].

neutral molecule. Each malonate ligand acts simultaneously as a chelating and bridging ligand. Here, the supramolecular interaction is different. During crystallization, the supramolecular interaction favors the coordination of the two carboxylate oxygens to another metal by replacing its water molecules. Thus, each zinc atom has three malonate units around its coordination sphere, one as bidentate and two as monodentates. The other two bondings are

provided by a water molecule and a piperazine molecule occurring *trans* to each other (Fig. 4). The structure can also be visualized as a 2-D CP sheet being pillared by piperazine molecules. The assembly also favors hydrogen bonding between coordinated water and the adjacent carboxylate oxygens (H2W···O1: 1.916(5) Å; H1W···O3: 1.974(4) Å). The average Zn–O bond length for the chelating malonate ligand is 2.092 Å while that for the bridging malonate is 2.135 Å. The assembly is further stabilized by N–H···O interaction (H1–O4: 2.226(4) Å).

Crystal structure of [{$CoCl_4$}{H_2pip}], 5

Retrosynthesis of the molecular solid **5**, shows that the structure is built of two tectons, viz., a discrete tetrahedral anion, $\{CoCl_4\}^{2-}$ and $\{H_2pip\}^{2+}$. The bond distances in $\{CoCl_4\}^{2-}$ are consistent with known tetrachlorocobaltate(II) complexes[22,23]. Strong hydrogen bonding interactions, N−H···Cl and C−H···Cl facilitate alternate zig-zag arrangement of $\{CoCl_4\}^{2-}$ and $\{H_2pip\}^{2+}$ units as shown in Fig. 5. It should be noted that crystal structure of **5** has been reported earlier by Decaroli *et al*.[24]

Crystal structure of [{Co(mal)(H_2O)(Hpip)}]Cl, 6

The nonmolecular solid **6** is an example of a 2-D CP, like the zinc compound, **4**, but with slight variation (Fig. 6). Unlike **4**, the piperazine moiety is protonated and hence cannot coordinate with the metal on the adjacent sheet. The piperazine molecule lies on a mirror plane and its nitrogen atom is disordered. Although the crystal symmetry in **6** restricts the refinement of position of carbon atoms belonging to piperazine on a plane, the thermal vibrations of the carbon atoms suggest a slightly staggered conformation. The overall composition of the lamellar sheet is $[Co(mal)(H_2O)(Hpip)]^+$ and hence requires a counter anion, Cl^-. The neighboring cationic sheets are stabilized by N−H···Cl interactions (average N2−Cl is ~3.076 Å).

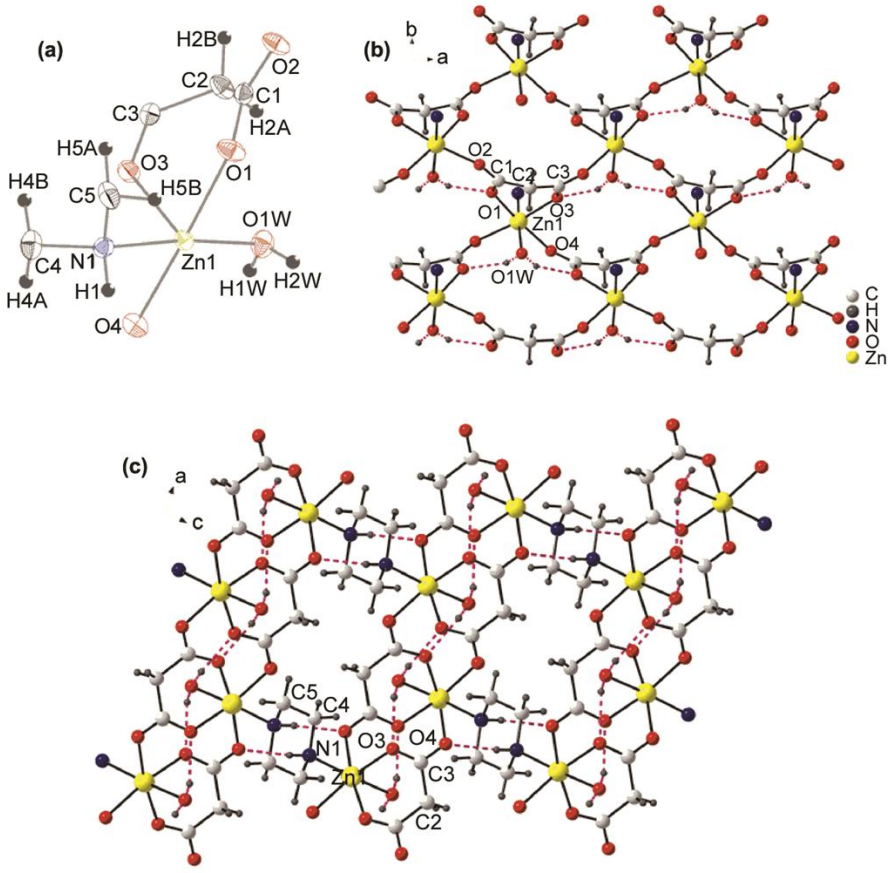

Fig. 4 – (a) ORTEP view of **4**, (b) view along *c*-axis showing 2-D CP {Zn(mal)(H_2O)}. [Hydrogen bonding (shown in dashed purple lines) between coordinated oxygen of carboxylate groups, O1 and O3 with water molecule (O1W) on metal center], and, (c) view along *b*-axis showing 2-D CP pillared by pip moieties. [N–H···O interaction further stabilizes the crystal structure].

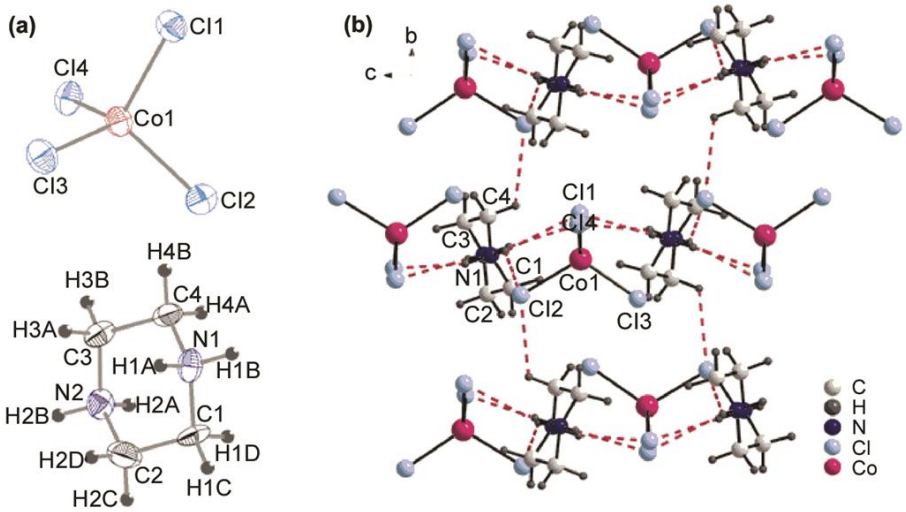

Fig. 5 – (a) ORTEP view of **5**, and, (b) crystal packing of the anion and cation in **5** is dictated by N−H···Cl and C−H···Cl interactions (shown in dashed purple lines).

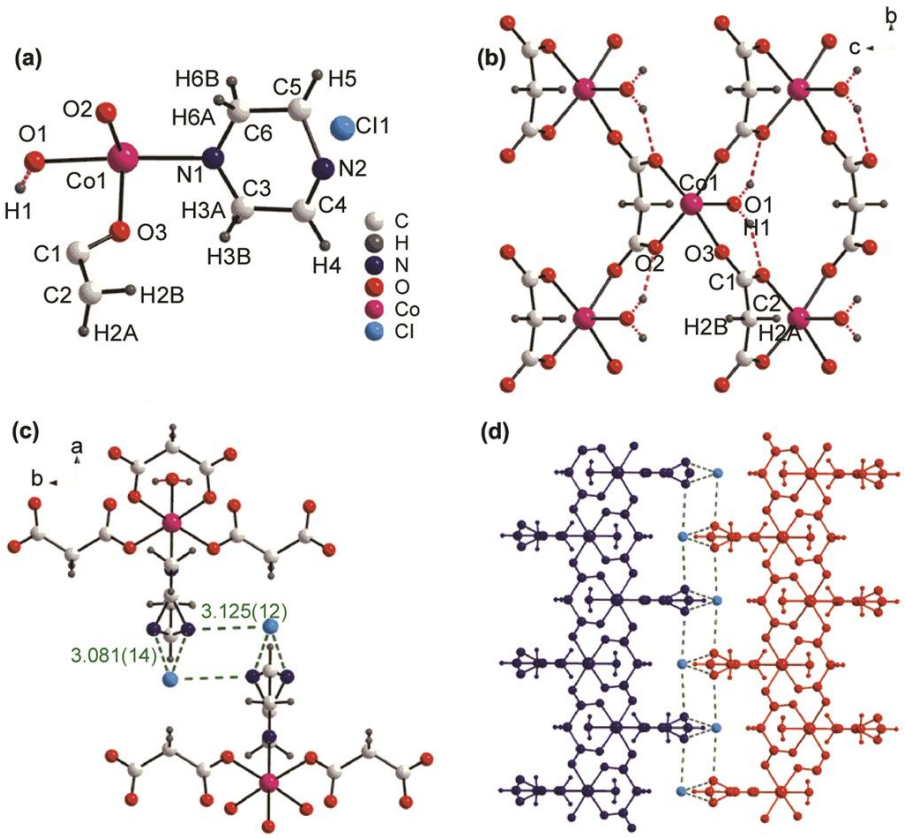

Fig. 6 – (a) Asymmetric unit in **6**, (b) view along *a*-axis showing 2-D CP $[Co(mal)(H_2O)(Hpip)]^+$ stabilized by hydrogen bonding interaction similar to **5**, (c) view along *c*-axis showing hydrogen bonding interaction between protonated piperazine and chloride ions, and, (d) stacking of two adjacent sheets (depicted in blue and red color) is facilitated by N−H···Cl interactions.

Chemistry of formation

Retrosynthesis provides molecular insights into the crystal syntheses of the coordination solids **1**-**6**. If a crystal is viewed as a supermolecule, crystallization is a supramolecular reaction[25]. Nucleation of a crystal occurs from chemically reasonable molecules or tectons, interacting in the solution at supersaturation. Retrosynthesis of a crystal structure suggests the possible molecular species involved in the supramolecular aggregation. As soon as metal chlorides are dissolved soluble species are formed; hence forth referred to as tectons (Scheme 2)[26,27]. Depending on the pH of the medium, the nature of the tectons differs. Crystallization is a supramolecular reaction. Every crystal assembled from a solution can in principle be controlled by judicious choice of reaction condition. Under highly acidic conditions, the tetrahedral tecton $\{CoCl_4\}^{2-}$ dominates the crystallization along with diprotonated piperazinium cation, hence solid **5** is crystallized. Under these conditions, malonic acid does not ionize and hence it does not complex with metal ions. In basic medium (pH > 7), hydroxide based tectons dominate, leading to the precipitation of basic or hydrated solids.

However, at pH ~5–7 ionization of malonic acid (pK_a = 2.83, 5.69) and the availability of protonated as well unprotonated piperazine moieties (pK_a = 5.68, 9.82) are significantly favored leading to interesting supramolecular reaction. Crystallization of the molecular solids **1**–**3** is not surprising though the geometry of the copper tecton necessitates the incorporation of water into the solid (Scheme 3). The difference in the formation of the sheets can be clearly seen. Thus, it can be concluded that molecular building blocks indeed play a very important role in the formation of such networks.

Occurrence of the 2-D coordination polymers, **4** and **6** with zinc and cobalt are interesting examples of supramolecular reactivity. In both cases, the cationic tecton is 1:1 metal to ligand complex. Since zinc hydrate is relatively more basic than the other hydrates, under similar condition, 1:2 complex is less favored. A choice of less polar solvent i.e., methanol probably leads to 1:1 complex tecton in the case of cobalt reaction. The malonate ligand with two uncoordinated carboxylate oxygens can interact with other such molecules to form a 2-D CP. In **6**, the combined effect of lesser availability of water molecules to form hydrogen bonded networks and the different solvation of malonate due to the hydrophobic interactions between the $–CH_2$ group of malonate and the $–CH_3$ group of methanol, possibly favor the formation of an extended framework that has malonate ligand in simultaneous bridging and chelating mode. As in the

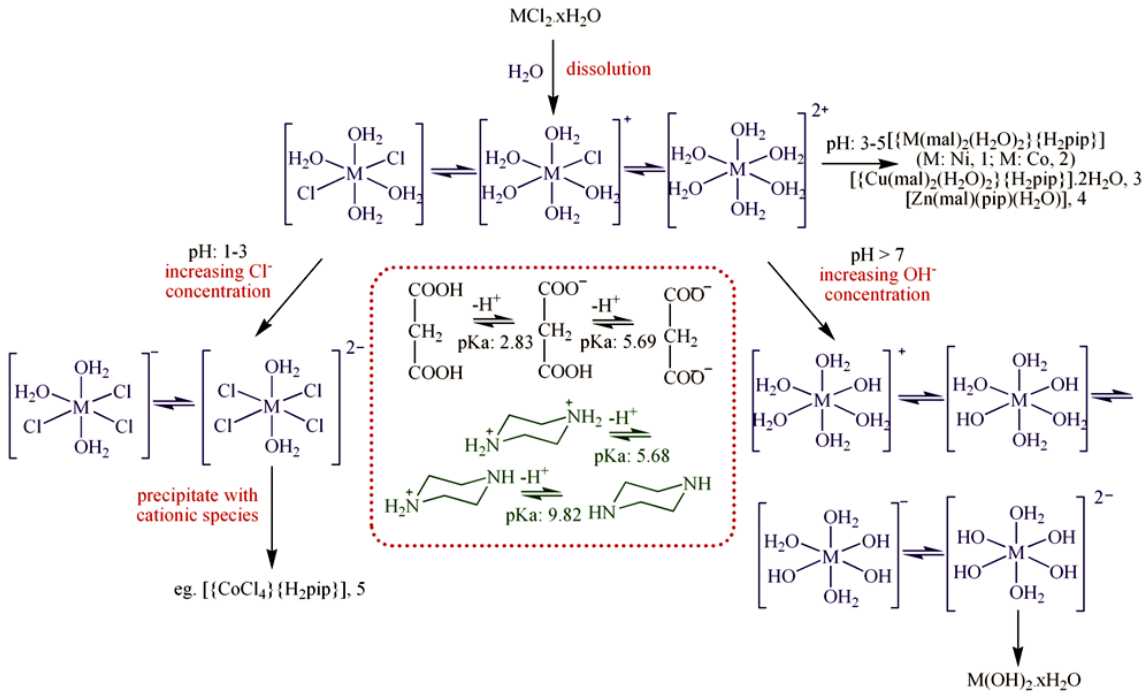

The dissolution of metal chlorides results in various tectons which aggregate with suitable counter ions to form solids **1-5**

Scheme 2

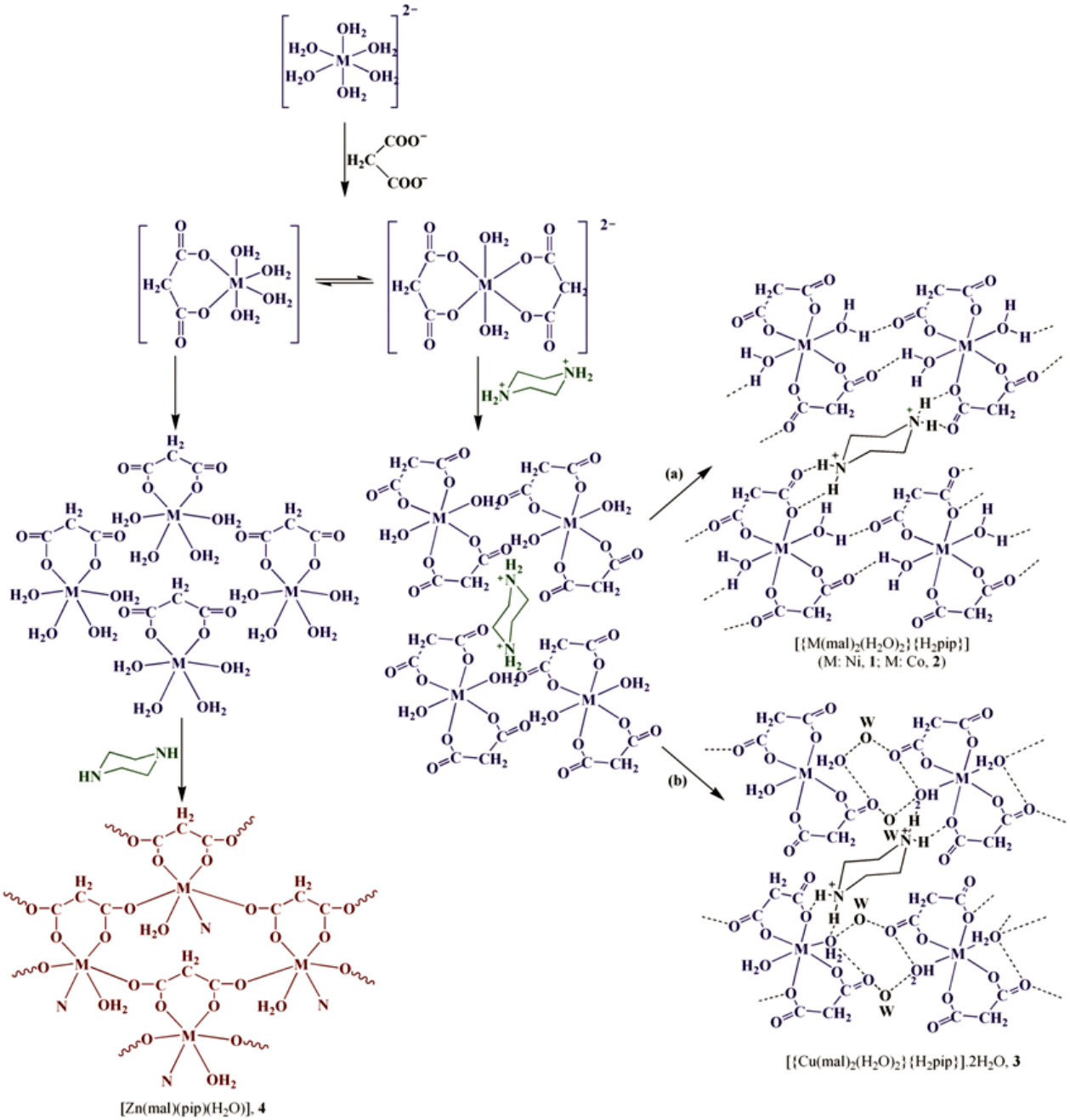

Supramolecular aggregation of tectons showing the formation of crystals **1-4**. Tecton $[M(H_2O)_6]^{2+}$ can either form a mono- or bi- ligated complex with $(mal)^{2-}$ leading to neutral $[M(mal)(H_2O)_4]$ or anionic $[M(mal)_2(H_2O)_2]^{2-}$ tectons. Thus, neutral $[M(mal)(H_2O)_4]$ tectons readily condense with neutral pip moieties to form **4**. On the other hand, anionic $[M(mal)_2(H_2O)_2]^{2-}$ tectons aggregate with $(H_2pip)^{2+}$ units. The self-assembly of $[M(mal)_2(H_2O)_2]^{2-}$ and $(H_2pip)^{2+}$ can therefore result in (a) **1** and **2** or (b) **3** upon inclusion of lattice water molecules.

Scheme 3

case of **4**, piperazine is now relatively free to coordinate to the metal center. However, the chloride ion being less stabilized in methanol is strongly hydrogen bonded to the protonated piperazine moiety, thereby restricting the coordination only to one metal.

Vibrational and thermal analysis

FTIR spectra of the solids exhibited broad bands around 3500–3550, 3400–3420 and 3100–3150 cm^{-1} were due to stretching vibrations of O–H of water, N–H and C–H groups of ligands. The bands from

1420 to 1640 cm^{-1} were assigned to bending vibrations of C–H, N–H and O–H (refer Supplementary Data, Table S3 for details)[28]. Although, solution FTIR has been employed for single component organic systems to probe its reaction mechanism; these data are not used in the case of simple metal complexes as they are too complicated to probe.

In all the cases, phase purity of the solids was established by comparing the experimental PXRD pattern with simulated powder pattern of the single crystal structure as shown in Figs S1–S4 (Supplementary Data). It was found that the cell parameters and space group from experimental powder data of bulk sample match well with the simulated single crystal parameters. The TGA of the solids are shown in Figs S5 and S6 (Supplementary Data). For solids **1** and **2**, the first two consecutive steps of weight loss occur in the temperature range of 50–180 and 200–250 °C, correspond to the release of coordinated water molecules and malonate moieties respectively. Subsequently piperazine moiety is lost which results in the final residue ~15% corresponding to nickel and cobalt in **1** and **2** respectively. The TGA curve of **3** is similar, which displays three consecutive steps of weight loss in the range of 50–480 °C (~85%) which can be attributed to the loss of water molecules, malonate moieties and piperazine. The residual solid can be attributed to elemental copper. While in the case of **4**, after the weight loss of water, malonate and piperazine moieties, only elemental zinc is left behind as residue; in **6** there are four consecutive steps of weight loss which can be attributed to the loss of water molecules, malonate, chloride and piperazine moieties. The resultant residue (~19%) corresponds to cobalt.

Conclusions

Exploration of the structural landscape of the system $\{M(H_2O)_n\}^{2+}$-mal-pip-H_2O, led to the synthesis of five new crystals. Retrosynthesis provides molecular insights into the crystallization of the different solids and links the supramolecular reaction occurring in the solution to the intermolecular interactions observable in the solid state. The examples demonstrate how by postulating chemically reasonable molecules (tectons), one can correlate the synthetic variables to the structures observed. The methodology described here also suggests the possibility of new phases in the system.

Supplementary Data

CCDC 717971-717974 (**1**–**4**), 857647 (**5**) and 720736 (**6**) contain the supplementary crystallographic data. These data can be obtained free of charge via http://www.ccdc.cam.ac.uk/conts/retrieving.html, or from the Cambridge Crystallographic Data Centre, 12 Union Road, Cambridge CB2 1EZ, UK; fax: (+44) 1223 336 033; or e-mail: deposit@ccdc.cam.ac.uk. Other supplementary data associated with this article are available in the electronic form at http://www.niscair.res.in/jinfo/ijca/IJCA_57A(8-9) 1081-1090_SupplData.pdf.

Acknowledgement

The results submitted herein are part of M. Sc. dissertation of Kaustubh R Mote. The authors thank Dr Shailesh Upreti, Senior Technology Advisor of Powerstorm Holdings, Inc., for helpful discussion. AR acknowledges Dept. of Science & Technology, Govt of India, New Delhi, India, for financial support as well as X-ray diffraction facility to IIT Delhi.

References

1 Seth S, Savitha G & Moorthy J N, *Cryst Growth Des*, 18 (2018) 2129.
2 Karthik R & Natarajan S, *Cryst Growth Des*, 16 (2016) 2239.
3 Special issue on *Coordination Polymers/MOFs: Structures, Properties and Applications*, *Chem Plus Chem*, 81 (2016) 666-898.
4 Li D S, Wu Y P, Zhao J, Zhang J & Lu J Y, *Coord Chem Rev*, 261 (2014) 1.
5 Biradha K, Ramanan A & Vittal J J, *Cryst Growth Des*, 9 (2009) 2969.
6 Delgado F S, Lorenzo-Luís P, Pasán J, Cañadillas-Delgado L, Fabelo O, Hernández-Molina M, Lozano-Gorrín A D, Lloret F, Julve M & Ruiz-Pérez C, *CrystEngComm*, 18 (2016) 7831.
7 Powell J E & Johnson D K, *J Chromatog*, 44 (1969) 212.
8 Stone B S, Staples R J & LaDuca R L, *Inorg Chim Acta*, 446 (2016) 176.
9 Delgado F S, Sanchiz J, Ruiz-Pérez C, Lloret F & Julve M, *Cryst Eng Comm*, 6 (2004) 443.
10 Zheng Y Q, Zhai X S, Jin L, Zhu H L, Lin J L & Xu W, *Polyhedron*, 68 (2014) 324.
11 Stone B S R & LaDuca R L, *Inorg Chem Commun*, 43 (2014) 56.
12 Ghoshal D, Maji T K, Mallah T, Lu T, Mostafa G & Chaudhuri N R, *Inorg Chim Acta*, 358 (2005) 1027.
13 Hemamalini M, Muthiah P T, Butcher R J & Lynch D E, *Inorg Chem Commun*, 9 (2006) 1155.
14 Yilmaz V T & Senel E, *Trans Met Chem*, 29 (2004) 336.
15 Ruiz-Pérez C, Sanchiz J, Hernández-Molina M, Lloret F & Julve M, *Inorg Chem*, 39 (2000) 1363.
16 Delgado F S, Sanchiz J, Ruiz-Pérez C, Lloret F & Julve M, *Cryst Engg Comm*, 5 (2003) 280.
17 *SMART: Bruker Molecular Analysis Research Tool*, *Ver. 5.618*, (Bruker Analytical X-ray Systems, USA), 2000.

18 *SAINT-NT, Ver. 6.04*, (Bruker Analytical X-ray Systems, USA) 2001.

19 *SHELXTL-NT, Ver. 6.10*, (Bruker Analytical X-ray Systems, USA) 2000.

20 Klaus B, *DIAMOND, Ver. 1.2c*, (University of Bonn, Germany) 1999.

21 Tectons (the Greek word τεκτων for builder) are chemically reasonable molecules that induce assembly of aggregates with controlled geometries and specific nonbonding interactions. Tecton can vary from simple molecule such as H_2O to robust unit like metal complex or any molecular ion. A tecton will be obvious in a molecular solid but it needs to be deduced from a nonmolecular solid through retrosynthesis.

22 Girma K B, Lorenz V, Blaurock S & Edelmann F T, *Z Anorgan Allg Chem*, 631 (2005) 1419.

23 Wei D Y, Xie H Z & Zheng Y Q, *Z Kristallogr*, 220 (2005) 497.

24 Decaroli C, Arevalo-Lopez A M, Woodall C H, Rodriguez E E, Attfield J P, Parker S F & Stock C, *Acta Cryst*, B71 (2015) 20.

25 Desiraju G R, Vittal J J & Ramanan A, *Crystal Engineering - A Textbook*, (World Scientific, Singapore) 2011.

26 Singh M, Kumar D, Thomas J & Ramanan A, *J Chem Sci*, 122 (2010) 757.

27 Singh M, Thomas J & Ramanan A, *Aust J Chem*, 63 (2010) 565.

28 Nakamoto K, *Infrared and Raman Spectra of Inorganic and Coordination Compounds*, (John Wiley & Sons, Inc.) 2009.